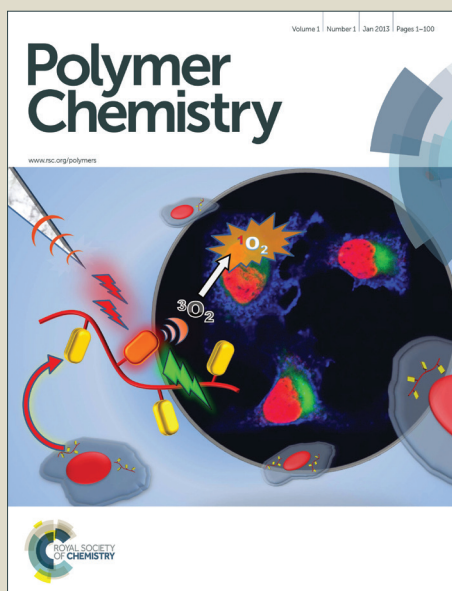


Polymer Chemistry

Accepted Manuscript



This is an *Accepted Manuscript*, which has been through the Royal Society of Chemistry peer review process and has been accepted for publication.

Accepted Manuscripts are published online shortly after acceptance, before technical editing, formatting and proof reading. Using this free service, authors can make their results available to the community, in citable form, before we publish the edited article. We will replace this *Accepted Manuscript* with the edited and formatted *Advance Article* as soon as it is available.

You can find more information about *Accepted Manuscripts* in the [Information for Authors](#).

Please note that technical editing may introduce minor changes to the text and/or graphics, which may alter content. The journal's standard [Terms & Conditions](#) and the [Ethical guidelines](#) still apply. In no event shall the Royal Society of Chemistry be held responsible for any errors or omissions in this *Accepted Manuscript* or any consequences arising from the use of any information it contains.

COMMUNICATION

Thermoresponsive Dual Emission Nanosensor Based on Quantum Dots and Dye Labeled Poly(N-isopropylacrylamide)

Cite this: DOI: 10.1039/x0xx00000x

Received 00th January 2012,
Accepted 00th January 2012Jinjun Zhou,^a Kaushik Mishra,^a Vrushali Bhagat,^a Abraham Joy^a and Matthew L. Becker^{*,a,b}

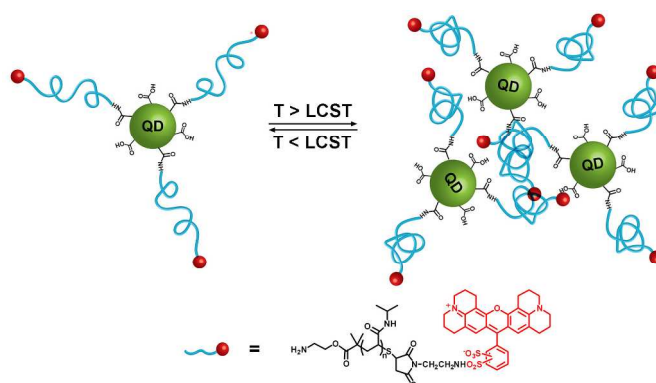
DOI: 10.1039/x0xx00000x

www.rsc.org/

Dual end-functionalized telechelic poly(N-isopropylacrylamide) (PNIPAM) was synthesized using reversible addition-fragmentation chain-transfer (RAFT) polymerization. One end was coupled to a fluorescent dye and the other end was covalently coupled to CdSe/ZnS quantum dots (QDs) through carbodiimide chemistry. The hybrid nanoparticle shows ratiometric changes in fluorescence emission upon temperature cycling between 25°C and 45°C.

Inorganic nanomaterials have been used to create stimuli responsive organic-inorganic sensors and probes for biological, environmental and safety applications.¹ A number of sensors based on gold nanoparticles², silver nanoparticles³, carbon nanotubes⁴ and quantum dots⁵ (QDs) have shown sensitivity to pH⁵, temperature^{2b}, ions^{2a, 2c, 3, 6} or other molecules^{2d, 4}. Among nanomaterials, QDs are an attractive choice due to their unique electrochemical and photophysical properties^{1a} such as tunable and intense absorption spectra, narrow-symmetric emission with high quantum yield, size-tunable, large “effective” Stokes shifts, high photostability and easy surface functionalization.^{1a, 7}

Sensors based on fluorescence resonance energy transfer (FRET) mechanism utilizing QDs as donors afford several inherent photophysical advantages. When compared to organic dyes, the advantages include the ability to optimize the spectral overlap by tuning the QD size, attaching multiple acceptors onto the QD surface and reducing the direct excitation of the acceptor.⁸ Dual-emitting QDs FRET sensors show enhanced detectivity and sensitivity.⁹ The combination of QDs and polymers has been used to prepare hybrid materials responsive to temperature or pH.^{5a, 10} Although dual-emitting QDs/polymer hybrid sensors have been reported, surface initiated polymerization is afflicted with poor molecular mass control and QDs designed as acceptors limit their application.^{5b} Here, a new method is proposed to prepare a QDs/polymer-based FRET sensor that precisely controls the molecular mass of the polymer and use QDs as the donor. PNIPAM with its lower critical solution temperature (LCST) of ~32 °C is probably the most-studied temperature responsive polymer,^{10c} and thus it is used in this work as a model polymer to prepare a temperature responsive sensor. Scheme 1 shows the structure and temperature response mechanism of the sensor. PNIPAM was synthesized by RAFT mediated

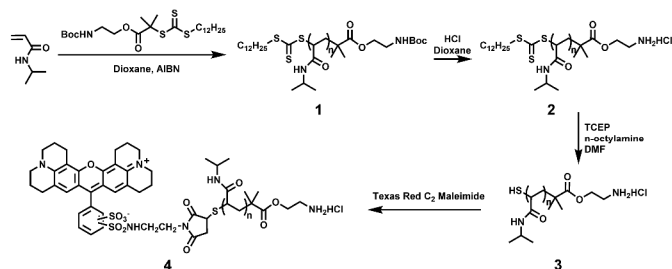


Scheme 1. Schematic of the FRET QDs/PNIPAM temperature sensor.

polymerization with precisely controlled molecular mass and dual-end functionality.¹¹ One end is a reactive group that is able to form a covalent bond to the QDs surface, while the other end is functionalized with a dye (Texas Red, TR). The molecular mass of PNIPAM was carefully selected for optimal dimensional spacing between the donor and acceptor to yield efficient FRET from QDs to the dye. When the temperature is lower than LCST, the polymer is hydrophilic and the chains are in a relatively extended conformation. When the conjugate is above the LCST, the polymer becomes hydrophobic and the chains collapse, resulting in a closer distance between QDs and dye. Since FRET efficiency is closely related to the distance between donor and acceptor,¹² changes in the QD and dye emission bands will be observed as a result of temperature change. Thus, a temperature response of the nanohybrid can be achieved by the ratio of the two emission bands.

Scheme 2 shows the synthesis route for the dual-end functionalized PNIPAM. The polymer was synthesized by RAFT polymerization in dioxane using 2-((tert-butoxycarbonyl)amino)ethyl 2-(((dodecylthio)carbonothioyl)thio)-2-methylpropanoate as the chain transfer agent. As a living polymerization technique, RAFT polymerization can be used to prepare polymers with controlled molecular mass by carefully choosing the ratio between the monomer, initiator and chain transfer

agent. Post-polymerization the two ends of polymer chain can be modified with different functional groups.



Scheme 2. Synthesis of dual end-functionalized PNIPAM via RAFT using a Boc-protected amine chain transfer agent.

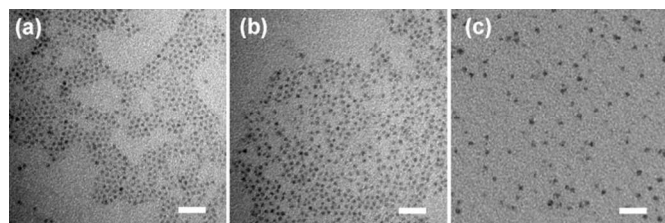


Fig. 1 TEM images of (a) TOPO/HDA coated QDs, (b) DHLA coated QDs, and (c) QDs-PNIPAM-TR. The scale bar is 25 nm.

A modified RAFT agent bearing a Boc protected amine group was used to synthesize PNIPAM (1) which was subsequently deprotected with HCl/dioxane to yield polymer (2). Aminolysis of trithiocarbonate with *n*-octylamine generated free thiol groups on the other end of the polymer (3). Texas Red (TR) was attached to the polymer chain via thio-ene reaction between the thiol group and Texas Red C₂ maleimide to obtain dual end functionalized PNIPAM (4). The successful synthesis of 4 was confirmed by UV-visible spectroscopy and mass spectroscopy (Fig. S6, Fig. S7, ESI). Detailed synthesis and characterization are listed in the supporting information.

QDs used in this study are core-shell CdSe/ZnS QDs and are synthesized using reported synthesis routes based on growth and annealing of organometallic compounds at high temperature.¹³ QDs with tunable size and absorption/photoluminescence spectra can be synthesized by using different experimental conditions. Ligand exchange with dihydrolipoic acid (DHLA) rendered the QDs water soluble via carboxylic functional groups. The QDs-PNIPAM-TR hybrid was prepared by covalently tethering PNIPAM-TR to the QDs surface through carbodiimide mediated amide coupling.

Fig. 1 shows TEM images of as synthesized organic coated QDs, DHLA coated water soluble QDs and QDs-PNIPAM-TR nanohybrid. Fig. 1a and 1b indicate that the QDs have narrow size distribution and are dispersed well both before and after ligand exchange. The size of TOPO/HDA (triethylphosphine oxide/hexadecylamine) covered core-shell QDs was determined to be 3.4±0.3 nm from TEM images. DHLA coated QDs have an average diameter of 3.5±0.4 nm. After the polymer was functionalized onto QDs surface, the hybrid can be dispersed well in aqueous solution without aggregate formation (Fig. 1c). The size of the hybrid increased to 4.2±0.5 nm due to the polymer coating on QDs surface.

FRET efficiency is dictated by the overlap between donor emission and acceptor absorption spectra,¹⁴ thus the size of QDs were carefully tuned such that the donor emission overlaps with the absorption band of TR. The distance between donor unit and acceptor unit also influence the FRET process.

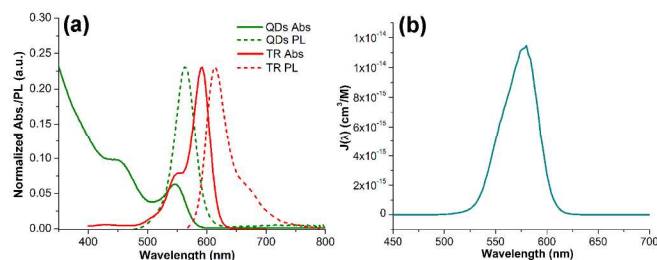


Fig. 2 (a) Normalized absorption and photoluminescence spectra of QDs and Texas Red. (b) Overlap function: $J(\lambda) = PL_{D-corr}(\lambda) \times \lambda^4 \times \epsilon_A(\lambda)$.

The normalized absorption and photoluminescence spectra are shown in Fig. 2a. Fig. 2b shows the overlap function $J(\lambda)$ between QDs and TR. It is used to calculate the Förster distance (R_0) with the following equation:^{12, 15}

$$R_0 = \left(\frac{9000(\ln 10) \kappa_p^2 Q_D}{N_A 128 \pi^5 n_D^4} I \right)^{1/6}$$

where $\kappa_p^2 = 2/3$ for randomly oriented dipoles, Q_D is the quantum yield of QDs, N_A is Avogadro's number, n_D is refractive index of medium. I is overlap integral, defined as $I = \int_0^\infty PL_{D-corr}(\lambda) \times \lambda^4 \times \epsilon_A(\lambda) d\lambda$, where PL_{D-corr} is a function of normalized donor emission spectrum, ϵ_A is extinction coefficient of acceptor. The FRET distance (R_0) of QDs and TR was calculated to be 40 Å. To have efficient FRET, the distance between donor and acceptor should be close to the 40 Å Förster distance. In this study, the molecular mass of PNIPAM was controlled by RAFT polymerization to be 5 kD. The end to end distance of the polymer chain is calculated to be 20 Å, making the center to center distance between QDs donor and TR acceptor to be 37.5 Å (see ESI for detailed calculation). This distance ensures an effective FRET to occur between QDs and TR.

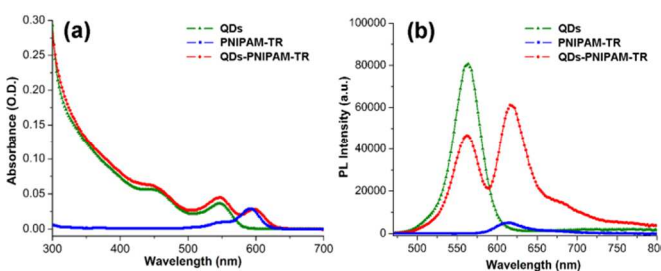


Fig. 3 Absorbance (a) and photoluminescence (b) spectra of QDs, PNIPAM-TR and QDs-PNIPAM-TR nanohybrid.

Fig. 3a shows the absorption spectra of QDs, PNIPAM-TR and QDs-PNIPAM-TR, while Fig. 3b shows their photoluminescence spectra. Excitation wavelength was chosen to be 400 nm for all the photoluminescence tests. The absorption spectrum of QDs-PNIPAM-TR hybrid is a superposition of that of QDs and PNIPAM-TR, which indicates the TR functionalized PNIPAM has been successfully introduced onto the QDs surface through amide covalent bond formation. The emission peak of QDs with a λ_{max} at 564 nm overlaps with the absorption spectrum of TR. The overlap

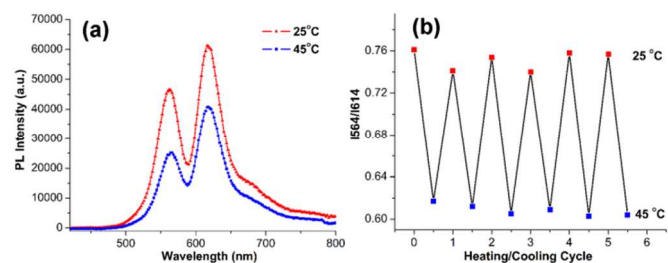


Fig. 4 (a) Photoluminescence spectra of QDs-PNIPAM-TR hybrid solution tested at 25 °C and 45 °C. (b) Reversible Photoluminescence intensity change (I564/I614) as a function of temperature shows a highly reproducible and stable response.

ensures FRET will happen between the QDs and TR where the QDs are a donor and TR is an acceptor. Fig. 3b shows that the emission intensity of TR from PNIPAM-TR is relatively low when excited at 400 nm, where TR has very limited absorption (Fig. 2a). For the hybrid material, the spectrum shows two strong emission bands; the peak at 564 nm is from QDs, while the one at 614 nm is assigned to TR. The intensity of QDs emission peak decreases, while at the same time the intensity of TR emission increases dramatically. Since the concentrations of TR in PNIPAM-TR and QDs-PNIPAM-TR are the same (Fig. 3a, same absorbance at 614 nm for PNIPAM-TR and QDs-PNIPAM-TR), the increase of TR emission peak intensity is a result of FRET between QDs and TR. These results show that the QD-PNIPAM-TR hybrid has been successfully prepared and FRET process occurs between QDs and TR due to careful selection of QDs, dye material, and PNIPAM polymer with precisely controlled molecular mass.

To test temperature response, the emission spectra of the hybrid material at 25 °C and 45 °C were recorded using an excitation wavelength of 400 nm. Since the LCST of PNIPAM is around 32 °C, 45 °C was chosen to investigate the hybrid's temperature response above LCST. Fig. 4a shows Photoluminescence (PL) spectra of the hybrid solution at 25 °C and 45 °C. When the temperature is raised from 25 °C to 45 °C, the emission from QDs at 564 nm decreases, while the emission for TR also decrease. When temperature is higher than LCST, PNIPAM chains become hydrophobic and collapse, resulting in a smaller distance between QDs and TR. According to the FRET theory, a smaller distance between donor and acceptor units will induce a higher FRET efficiency. For the QDs-PNIPAM-TR nanohybrid material, when temperature is above LCST, the shorter distance between QDs and TR will result in higher FRET efficiency, and hence the PL intensity of TR should increase. However, this was not observed for the nanohybrid prepared here. The PL intensity of TR for a mixture of QDs and PNIPAM-TR shows limited change upon temperature increase from 25 °C to 45 °C (Fig. S8).

The reason for decreased PL of TR in the nanohybrid has to be related to quenching effect of PNIPAM on QDs emission, which has been observed in other studies.^{1b, 10a} Nonetheless, the ratio of QDs and TR peak intensity (I564/I614) was used to monitor the temperature response of this hybrid. Fig. 4b shows how the ratio changes while temperature cycles between 25 °C to 45 °C. The results indicate a nearly reversible change of peak intensity ratios even after 5 cycles of temperature change. Thus QDs-PNIPAM-TR hybrid responds to change in temperature and might be used as a temperature sensor.

To better understand the nanohybrid material upon temperature changes, dynamic light scattering (DLS) was used

to determine the hydrodynamic diameters (D_h). Fig. 5 shows size distribution histograms of DHLA coated QDs and QDs-PNIPAM-TR nanohybrid (measured at 25 °C and 45 °C). The DLS results showed that D_h of DHLA coated QDs was 7.3 ± 1.9 nm and D_h of QDs-PNIPAM-TR under 25 °C was 17.1 ± 5.1 nm. After decoration with the polymer, the hydrodynamic diameter of the nanohybrid increased compared to that of QDs alone. The size was consistent with TEM results. The size of nanohybrid determined by DLS are somewhat larger than that measured by TEM, which is because nanohybrid in aqueous solution are hydrated and polymer chains are extended when temperature is below LCST. When temperature was increased to 45 °C, which was above LCST, D_h of QDs-PNIPAM-TR nanohybrid increased to 247 ± 109 nm, indicating the formation of aggregates. The aggregates can serve as scattering center, which could cause the PL intensity decrease of QDs inside the hybrid and this explains the quenching effect of PNIPAM on QDs emission. The aggregation also affects the distance between the QDs and dye, and hence the FRET between them. Although the effect of aggregates on PL was complicated, temperature sensing was still achieved by comparing the two PL peak intensities and a nearly reversible change was observed.

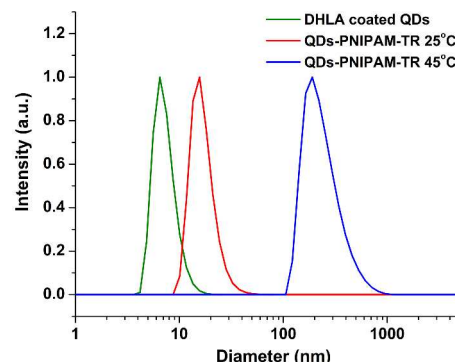


Fig. 5 Size distribution histogram of DHLA coated QDs and QDs-PNIPAM-TR (at 25 °C and 45 °C) measured by DLS.

In summary, a new strategy is demonstrated to prepare sensors based on QD nanoparticles-decorated with stimuli-responsive polymers. Using RAFT polymerization, dual-end functionalized polymers were synthesized with precisely controlled molecular mass and conjugated to a fluorescent dye as the reporter and to QD nanoparticles as FRET donors. The current methodology is versatile and can be extended to other stimuli responsive polymers to tune both the temperature range and potentially the external stimulus for other QD based sensors.

Notes and references

^a Department of Polymer Science, The University of Akron, Akron, Ohio 44325, United States.

^b Department of Biomedical Engineering, The University of Akron, Akron, Ohio 44325, United States.

Electronic Supplementary Information (ESI) available: experimental details, synthesis of QDs and dual-end functionalized PNIPAM, and characterization data. See DOI: 10.1039/c000000x/

1 (a)D. E. Prasuhn, A. Feltz, J. B. Blanco-Canosa, K. Susumu, M. H. Stewart, B. C. Mei, A. V. Yakovlev, C. Loukou, J.-M. Mallet, M.

- Oheim, P. E. Dawson and I. L. Medintz, *ACS Nano*, 2010, **4**, 5487; (b) O. Tagit, D. Jańczewski, N. Tomczak, M. Y. Han, J. L. Herek and G. J. Vancso, *Eur. Polym. J.*, 2010, **46**, 1397; (c) C. Li, J. Hu and S. Liu, *Soft Matter*, 2012, **8**, 7096.
- 2 (a) J. Liu and Y. Lu, *J. Am. Chem. Soc.*, 2003, **125**, 6642; (b) M.-Q. Zhu, L.-Q. Wang, G. J. Exarhos and A. D. Q. Li, *J. Am. Chem. Soc.*, 2004, **126**, 2656; (c) J.-S. Lee, M. S. Han and C. A. Mirkin, *Angew. Chem., Int. Ed.*, 2007, **46**, 4093; (d) J. Liu and Y. Lu, *Angew. Chem., Int. Ed.*, 2006, **45**, 90.
- 3 G.-Y. Lan, C.-C. Huang and H.-T. Chang, *Chem. Commun.*, 2010, **46**, 1257.
- 4 (a) K. Besteman, J.-O. Lee, F. G. M. Wiertz, H. A. Heering and C. Dekker, *Nano Lett.*, 2003, **3**, 727; (b) J. Kong, M. G. Chapline and H. Dai, *Adv. Mater.*, 2001, **13**, 1384.
- 5 (a) K. Paek, H. Yang, J. Lee, J. Park and B. J. Kim, *ACS Nano*, 2014, **8**, 2848; (b) K. Paek, S. Chung, C.-H. Cho and B. J. Kim, *Chem. Commun.*, 2011, **47**, 10272; (c) X. Ji, G. Palui, T. Avellini, H. B. Na, C. Yi, K. L. Knappenberger and H. Mattoussi, *J. Am. Chem. Soc.*, 2012; (d) Y. Wu, S. Chakraborty, R. A. Gropeanu, J. Wilhelmi, Y. Xu, K. S. Er, S. L. Kuan, K. Koynov, Y. Chan and T. Weil, *J. Am. Chem. Soc.*, 2010, **132**, 5012; (e) T. Jin, A. Sasaki, M. Kinjo and J. Miyazaki, *Chem. Commun.*, 2010, **46**, 2408; (f) I. L. Medintz, M. H. Stewart, S. A. Trammell, K. Susumu, J. B. Delehanty, B. C. Mei, J. S. Melinger, J. B. Blanco-Canosa, P. E. Dawson and H. Mattoussi, *Nat. Mater.*, 2010, **9**, 676.
- 6 A. Zhu, Q. Qu, X. Shao, B. Kong and Y. Tian, *Angew Chem Int Ed Engl*, 2012, **51**, 7185.
- 7 (a) W. R. Algar, K. Susumu, J. B. Delehanty and I. L. Medintz, *Anal. Chem.*, 2011, **83**, 8826; (b) J. M. Klostranec and W. C. W. Chan, *Adv. Mater.*, 2006, **18**, 1953; (c) X. Michalet, F. F. Pinaud, L. A. Bentolila, J. M. Tsay, S. Doose, J. J. Li, G. Sundaresan, A. M. Wu, S. S. Gambhir and S. Weiss, *Science*, 2005, **307**, 538.
- 8 K. Boeneman, B. C. Mei, A. M. Dennis, G. Bao, J. R. Deschamps, H. Mattoussi and I. L. Medintz, *J. Am. Chem. Soc.*, 2009, **131**, 3828.
- 9 (a) A. E. Albers, E. M. Chan, P. M. McBride, C. M. Ajo-Franklin, B. E. Cohen and B. A. Helms, *J. Am. Chem. Soc.*, 2012, **134**, 9565; (b) M. Suzuki, Y. Husimi, H. Komatsu, K. Suzuki and K. T. Douglas, *J. Am. Chem. Soc.*, 2008, **130**, 5720.
- 10 (a) Y.-Q. Wang, Y.-Y. Zhang, F. Zhang and W.-Y. Li, *J. Mater. Chem.*, 2011, **21**, 6556; (b) J. Ye, Y. Hou, G. Zhang and C. Wu, *Langmuir*, 2008, **24**, 2727; (c) D. Jańczewski, N. Tomczak, M.-Y. Han and G. J. Vancso, *Macromolecules*, 2009, **42**, 1801.
- 11 (a) P. J. Roth, K.-S. Kim, S. H. Bae, B.-H. Sohn, P. Theato and R. Zentel, *Macromol. Rapid Commun.*, 2009, **30**, 1274; (b) P. J. Roth, M. Haase, T. Basché, P. Theato and R. Zentel, *Macromolecules*, 2009, **43**, 895; (c) S. W. Hong, D. Y. Kim, J. U. Lee and W. H. Jo, *Macromolecules*, 2009, **42**, 2756.
- 12 J. R. Lakowicz, *Principles of Fluorescence Spectroscopy*, Springer, New York, 2006.
- 13 (a) B. O. Dabbousi, J. Rodriguez-Viejo, F. V. Mikulec, J. R. Heine, H. Mattoussi, R. Ober, K. F. Jensen and M. G. Bawendi, *J. Phys. Chem. B*, 1997, **101**, 9463; (b) Z. A. Peng and X. Peng, *J. Am. Chem. Soc.*, 2001, **123**, 183.
- 14 X. Wan and S. Liu, *J. Mater. Chem.*, 2011, **21**, 10321.
- 15 A. R. Clapp, I. L. Medintz, J. M. Mauro, B. R. Fisher, M. G. Bawendi and H. Mattoussi, *J. Am. Chem. Soc.*, 2003, **126**, 301.

For Table of Contents use only:

